Chylomicron remnants are increased in the postprandial state in CD36 deficiency

Daisaku Masuda,[1,*] Ken-ichi Hirano,[†] Hiroyuki Oku,[†] Jose C. Sandoval,[†] Ryota Kawase,[§] Miyako Yuasa-Kawase,[†] Yasushi Yamashita,[**] Masanori Takada,[§] Kazumi Tsubakio-Yamamoto,[†] Yoshihiro Tochino,[*] Masahiro Koseki,[†] Fumihiko Matsuura,[†] Makoto Nishida,[††] Toshiharu Kawamoto,[**] Masato Ishigami,[§§] Masatsugu Hori,[†] Iichiro Shimomura,[*] and Shizuya Yamashita[†]

Departments of Metabolic Medicine,[*] Cardiovascular Medicine,[†] and Biomedical Informatics,[§§] Osaka University Graduate School of Medicine, 2-2 Yamada-oka, Suita, Osaka 565-0871, Japan; Department of Cardiology,[§] Kawasaki Hospital, 3-3-1 Higashiyama-cho, Hyogo Ward, Kobe, Hyogo 652-0042, Japan; Department of Cardiology,[**] Kure Heart Center, National Hospital Organization Kure Medical Center, 3-1 Aoyama-cho, Kure, Hiroshima 737-0023, Japan; and Health Care Center,[††] Osaka University, 1-7 Machikaneyama, Toyonaka, Osaka 560-0043, Japan

Abstract **The clustering of risk factors including dyslipidemia, hyperglycemia, and hypertension is highly atherogenic along with the excess of remnants from triglyceride (TG)-rich lipoproteins. CD36 is involved in the uptake of long-chain fatty acids (LCFAs) in muscles and small intestines. Patients with CD36 deficiency (CD36-D) have postprandial hypertriglyceridemia, insulin resistance, and hypertension. To investigate the underlying mechanism of postprandial hypertriglyceridemia in CD36-D, we analyzed lipoprotein profiles of CD36-D patients and CD36-knockout (CD36-KO) mice after oral fat loading (OFL). In CD36-D patients, plasma triglycerides, apolipoprotein B-48 (apoB-48), free fatty acids (FFAs), and free glycerol levels were much higher after OFL than those of controls, along with increases in chylomicron (CM) remnants and small dense low-density lipoprotein (sdLDL) particles. In CD36-KO mice, lipoproteins smaller than CM in size in plasma and intestinal lymph were markedly increased after OFL and mRNA levels of genes involved in FFA biosynthesis, such as fatty acid binding protein (FABP)-1 and FAS, were significantly increased. These results suggest that CD36-D might increase atherosclerotic risk by enhancing plasma level of CM remnants due to the increased synthesis of lipoproteins smaller than CM in size in the intestine.—** Masuda, D., K. Hirano, H. Oku, J. C. Sandoval, R. Kawase, M. Yuasa-Kawase, Y. Yamashita, M. Takada, K. Tsubakio-Yamamoto, Y. Tochino, M. Koseki, F. Matsuura, M. Nishida, T. Kawamoto, M. Ishigami, M. Hori, I. Shimomura, and S. Yamashita. **Chylomicron remnants are increased in the postprandial state in CD36 deficiency. *J. Lipid Res.* 2009.** 50: **999–1011.**

Supplementary key words atherosclerosis • apolipoprotein B-48 • free fatty acids • free glycerol • TG-rich lipoproteins • small dense LDL

In recent years, the clustering of coronary risk factors such as dyslipidemia, hyperglycemia, and hypertension related to abdominal obesity has been called the "metabolic syndrome" (MetS) and is a problem all over the world. Recently, several epidemiological studies have demonstrated that hypertriglyceridemia is closely related to the development of atherosclerosis (1, 2). Excess triglyceride (TG)-rich lipoproteins (TRLs), such as chylomicrons (CMs) or VLDLs, appear to be associated with the formation of atheroma. In particular, partially catabolized TRLs in the form of remnant lipoprotein particles (RLPs) are considered to be highly atherogenic (3–5). Plasma RLP-cholesterol (RLP-C) levels have been shown to be associated with an increased risk of coronary heart disease and related to insulin resistance and type II diabetes mellitus (6).

CD36, one of the class B scavenger receptors, is an 88 kDa glycoprotein and expressed on a variety of cells/tissues, such as platelets, monocytes/macrophages, intestinal cells, microvascular endothelial cells, smooth muscle cells, adipose tissues, skeletal muscles, and cardiomyocytes (7). It is well known that CD36 binds to long-chain fatty acids (LCFAs). CD36 is assumed to be associated with the uptake of LCFAs because the liver fatty acid binding protein (L-FABP, FABP1)

This work was supported by the following grants: a grant-in-aid for Scientific Research (No. 18659267) to S. Yamashita from the Ministry of Education, Science, Sports and Culture in Japan; a grant from Mitsui Life Social Welfare Foundation to S. Yamashita; a grant from Takeda Science Foundation to S. Yamashita; and an Osaka Heart Club Grant for Cardiovascular Disease to D. Masuda.

Manuscript received 14 September 2007 and in revised form 3 April 2008 and in re-revised form 29 July 2008 and in re-re-revised form 26 August 2008.

Published, JLR Papers in Press, August 27, 2008.
DOI 10.1194/jlr.P700032-JLR200

Abbreviations: apoB-48, apolipoprotein B-48; CM, chylomicron; FABP, fatty acid binding protein; FFA, free fatty acid; LCFA, long-chain fatty acid; LPL, lipoprotein lipase; MetS, metabolic syndrome; OFL, oral fat loading; TC, total cholesterol; TG, triglyceride; PL, phospholipids; RLP, remnant lipoprotein particle; sdLDL, small dense LDL; TRL, triglyceride-rich lipoprotein; WT, wild-type.

[1] To whom correspondence should be addressed.
e-mail: masuda@imed2.med.osaka-u.ac.jp

and intestinal fatty acid binding protein (I-FABP, FABP2) in the small intestine are colocalized with CD36 (8).

In 1990, a patient with CD36 deficiency (CD36-D) was found by Yamamoto et al. (7) to have a lack of antigen on platelets; of patients who were refractory to multiple platelet transfusions, several with mutations in the CD36 gene were identified in our laboratory. CD36-D is the only genetic deficiency state among scavenger receptors in humans. Furthermore, evaluation of the clinical phenotypes of patients with CD36-D indicated that they had the typical metabolic features of MetS, such as dyslipidemia including postprandial hypertriglyceridemia, insulin resistance, and hypertension (9, 10). These phenotypes have also been observed in CD36-KO mice (11, 12). Furthermore, we reported that plasma apolipoprotein B-48 (apoB-48) levels in the postprandial state were elevated with accumulation of TRL in patients with CD36-D (10), which might be one of the genetic models for MetS with hypertriglyceridemia (7).

Recently, several groups evaluated the mechanism of postprandial hyperlipidemia in CD36-KO mice (13, 14). Drover et al. (13) reported that the intestinal uptake of LCFA was not impaired in CD36-KO mice and that lipid droplets were extremely evident in the intestines of CD36-KO mice fed a high-fat diet ad libitum. Furthermore, they showed that after an oral loading of fat containing [^{3}H] labeled TG, the radioactivity of lymph drained from the intestine was lower in CD36-KO mice compared with wild-type (WT) mice. They concluded that the postprandial hyperlipidemia in CD36-KO mice was caused by impaired clearance of intestine-derived TRLs from the peripheral tissue even though the TG secretions from the intestine were decreased. Moreover, Goudriaan et al. (14) speculated that the impaired clearance of TRLs in CD36-KO mice might be due to the inhibition of lipoprotein lipase (LPL) by high concentrations of FFAs. Their results could explain one aspect of the postprandial hyperlipidemia in CD36-KO mice; however, when we evaluated the postprandial lipid profiles of the intestine-derived lymph, we got the opposite result that TG level of the intestinal lymph in CD36-KO mice was more increased after OFL compared with WT mice and hypothesized that the intestinal TG production was not impaired, but rather increased in CD36-KO mice.

Although we have clearly demonstrated the accumulation of TRLs in patients with CD36-D, the underlying mechanism for postprandial hypertriglyceridemia has not yet been clarified. In this study, we examined fasting and postprandial lipid profiles in patients with CD36-D. Furthermore, in CD36-KO mice, we examined plasma lipid profiles after OFL, hepatic VLDL production, and intestinal CM production, and the gene expression involved in the intestinal biosynthesis of FFAs and lipoproteins.

MATERIALS AND METHODS

Evaluation of metabolic phenotypes of patients with CD36-D

Among patients whose hearts were evaluated by single photon emission computed tomography at Osaka University Hospital and related hospitals, 40 patients without myocardial accumulation of an LCFA analog, ^{123}I-β-methyl-p-iodophenyl-pentadecanoic acid (^{123}I-BMIPP), and with the absence of CD36 antigen on monocytes or platelets, as determined by flow cytometry analysis performed after informed consent, were diagnosed with type I CD36 deficiency (CD36-D). Normal healthy volunteers (n = 84) matched for age, sex, and body mass index (BMI) served as controls. Each subject gave written informed consent before participating in the study, and the ethics committee of the Osaka University Hospital approved the study design. All samples were collected in accordance with the Helsinki Declaration. Blood pressure was determined in the sitting position, and peripheral venous blood was drawn while subjects were fasting. Serum total cholesterol (TC), TG, HDL-cholesterol, and fasting plasma glucose levels were measured by the enzymatic method; HbA1c levels were measured by the HPLC method (Dai-ichi Pure Chemicals, Chiba, Japan); and plasma adiponectin levels were determined using a human adiponectin ELISA kit (Otsuka Pharmaceuticals, Tokyo, Japan). Features of MetS were defined according to the Japanese guidelines for the diagnosis of MetS (15); *1*) fasting serum TG $\geq$ 150 mg/dl and/or fasting HDL-cholesterol level <40 mg/dl; *2*) systolic blood pressure $\geq$ 130 mmHg and/or diastolic blood pressure $\geq$ 85 mmHg; *3*) fasting serum glucose $\geq$ 110 mg/dl. The number of features of MetS was counted and compared.

OFL test of patients and controls

Four CD36-D patients and 12 normal healthy volunteers were loaded with OFTT cream (containing 35% fat without sugar, 30 g fat/m^2 body surface area, JOMO Foods, Japan) after overnight fasting. Blood was drawn before and at the indicated times (1–8 h) after OFL, followed by immediate serum and plasma separation with low-speed centrifugation. Concentrations of TC and free cholesterol, TG, HDL-cholesterol, FFAs, and phospholipids (PLs) were measured by the enzymatic method; apoAI, AII, B, CII, CIII, and E by the immunoturbidity method (Dai-ichi Pure Chemicals Co., Ltd., Tokyo, Japan); and apoB-48 by a sandwich chemiluminescent enzyme immunoassay (Fuji Rebio Inc., Tokyo, Japan) that we developed previously (16). For the evaluation of changes in remnant lipoproteins, we used the remnant lipoproteins cholesterol homogenous assay (RemL-C®, Kyowa Medex, Tokyo, Japan), which can determine CM and VLDL remnants with high specificity (17) and has a strong positive correlation with RLP-C concentrations at fasting (6). The fasting samples and those obtained 4 h after OFL were used for determination of free glycerol levels by the enzymatic method (Sigma-Aldrich, St Louis, MO). For the comparison of the net postprandial changes of these parameters, the incremental area under the curve (iAUC) of TG, apo B-48, FFA, and Reml-C was calculated.

Lipoprotein analysis by HPLC

The lipoprotein profile of the patients (n = 4) and controls (n = 12) during fasting and after OFL were analyzed by an online dual enzymatic method for simultaneous quantification by HPLC at Skylight Biotech Inc. (Akita, Japan), according to the procedure described by Usui et al. (18). Two hundred microliters of plasma were dissolved with the loading buffer and loaded into TSK gel Lipopropak XL columns. The concentrations of TC and TG in the flow-through were measured continuously and simultaneously (18) in the fasting state and 4 h after OFL. In the prior investigation of lipoproteins using the HPLC method, the correspondence of lipoprotein fractions (CM, VLDL, LDL, and HDL-sized fractions) and the elution time were already confirmed by comparing the HPLC pattern of representative lipoproteins separated by ultracentrifugation [CM (>80 nm, fraction time:

15–17 min), VLDL (30–80 nm, fraction time: 17–22 min), LDL (16–30 nm, fraction time: 22–28 min), and HDL (8–16 nm, fraction time: 28–37 min)] (18, 19). Small dense LDL (sdLDL), one of the atherogenic lipoproteins, was detected in each sample as a smaller-sized LDL fraction (estimated lipoprotein particle size: 16–25.5 nm, elution time: 25.2–28 min) (19). We evaluated TG and TC concentrations of these fractions and compared the LDL peak of TC concentration.

The flow-through was serially collected into 84 tubes according to elution time, with 150 μl of the flow-through collected in each tube. To confirm whether CM or its remnants were contained in each fraction, apoB48 protein was detected by Western blotting using anti-human apoB-48 antibody, which was provided by Fujirebio Inc. (Tokyo, Japan). From the tubes that were supposed to contain CM remnants (tubes No. 11, 14, 17, 20, 23, 26, 29, 32, 35), 15 μl of flow-through (containing ~10 μg protein) was taken, subjected to 4–12% SDS-polyacrylamide gel electrophoresis (SDS-PAGE, TEFCO, Tokyo, Japan) and transferred onto the Immobilon-P Transfer membrane (Millipore Corp., Billerica, MA). This membrane was incubated with anti-human apoB-48 antibody and subsequently with anti-mouse IgG antibody (NA931V, GE Healthcare, Backinghamshire, UK). The bands of apoB-48 were detected with the ECL Advance Detection Kit (GE Healthcare, Backinghamshire, UK). In addition, TG concentrations of CM remnant fractions in which apoB-48 protein was detected were measured in CD36-KO mice and WT mice.

Animals and diets

CD36-KO mice created on a C57BL6/J background were kindly provided by Mason. W. Freeman, MD, PhD, Professor of Harvard Medical School (20). CD36-KO and C57BL6/J mice (as WT) were housed in a temperature- and humidity-controlled facility with a 12-h light/dark cycle and fed a normal chow diet (MF, OrientalBio Laboratories, Chiba, Japan). All mice were male and 8–12 weeks of age, with body weights of 18–24 g. The experimental protocol was approved by the Ethics Review Committee for Animal Experimentation of Osaka University Graduate School of Medicine and was conducted in conformity with the Public Health Service (PHS) Policy on Humane Care and Use of Laboratory Animals, incorporated in the Institute for Laboratory Animal Research (ILAR) Guide for Care and Use of Laboratory Animals.

OFL test of CD36-KO and WT mice

After about 16 h of fasting, CD36-KO (n = 9) and WT (n = 8) mice were loaded with 17 μl/g body weight of olive oil (Nacalai Tesque, Kyoto, Japan) by gavage. Blood samples (15 μl) were drawn from the retro-orbital plexus into EDTA-containing tubes before and at the indicated times (1–8 h) after OFL. The plasma levels of TG, FFA, and free glycerol were measured by enzymatic methods. For the evaluation of the plasma lipoprotein profile of mice, an HPLC study was also performed. From CD36-KO (n = 6) and WT (n = 6) mice, 140 μl of blood was drawn from the retro-orbital plexus during fasting and 3 h after OFL. Plasma samples (15 μl) were injected into HPLC columns. TC, TG, and phospholipids (PLs) concentrations were calculated in the same manner as previously described.

Triton WR-1339 experiments during fasting and after OFL and postheparin lipase activity

Triton WR-1339 is a potent inhibitor of LPL and HL. In order to measure the secretion rate of lipoproteins from the intestines and the liver, triton WR-1339 (Nacalai Tesque, Kyoto, Japan) was injected during fasting (i) and after OFL (ii). CD36-KO (n = 4) and WT (n = 4) mice were used for both experiments. In experiment (i), we injected triton WR-1339 in the fasting state for the evaluation of lipoprotein secretion from the liver. To the contrary, in experiment (ii), after the injection of triton WR-1339, we performed OFL for the evaluation of the additional effect of lipoproteins derived from the small intestine. These experiments were different in the timing of triton WR-1339 injection from the similar experiment done by Drover et al. (13); they injected triton WR-1339 after OFL and concluded that there is little additional inhibition when injecting triton WR-1339 in CD36-KO. Blood was drawn from the retro-orbital plexus during fasting and after injection of triton WR-1339 (500 mg/kg) into the tail vein. In experiment (ii), mice were loaded with 17 μl olive oil /g body weight within a few minutes after the injection of triton WR-1339. Plasma TG levels were measured by the enzymatic method. ApoB-48 levels 2 and 4 h after OFL, in experiment (ii), were analyzed by Western blotting. Two microliters of plasma containing ~10 μg protein diluted with PBS were subjected to SDS-PAGE. ApoB-48 protein was detected using anti-mouse apoB-48/B-100 antibody (BIODESIGN International, Saco, ME) and anti-rabbit IgG antibody (NA934V, GE Healthcare, Backinghamshire, UK), followed by detection with the ECL Advance Detection Kit. Moreover, for the evaluation of LPL and HL activity, heparin (100 U/kg BW, Mochida Pharmaceutical Co., Ltd., Tokyo, Japan) was injected intravenously into the tail vein after 16 h fasting. Five minutes after injection, blood was drawn for measurement of lipase activity (21).

Histological analysis by Oil Red O staining and electron microscopic study

Intestinal tissues of CD36-KO (n = 4) and WT mice (n = 4) were obtained during fasting and 30 and 60 min after OFL. Mice were anesthetized by intraperitoneal injection of 1 mg pentobarbital sodium before the intestines were removed. The intestinal tissues were divided into three segments, and pieces of the oral side were washed with PBS and fixed with 4% paraformaldehyde by overnight incubation at 4°C and then with 30% sucrose overnight at 4°C. After segments were cryoembedded in Tissue-TeK O.C.T. compound (Sakura Finetechnical Co., Ltd., Tokyo, Japan), the sections were prepared by subsequent cryostat sectioning of 5 μm thicknesses and applied to MAS-coated SUPERFROST slides (Matsunami glass, Tokyo, Japan). The sections were stained with Oil Red O and hematoxylin and then observed with COOLSCOPE (Nikon, Tokyo, Japan). The intestines at the same position of Oil Red O staining were obtained, fixed by the injection of 2% glutaraldehyde and 1% osmium tetroxide, and stained by uranyl acetate. Ultrathin sections were made and examined with a Hitachi H-7100 electron microscope.

Lipid and lipoprotein analysis of intestinal lymph

CD36-KO (n = 4) and WT (n = 4) mice were loaded with olive oil (17 μl/g body weight) after 16 h fasting and anesthetized. A needle with a polyethylene tube (PE-50), which was filled with EDTA-treated water and hung to the floor, was cannulated into the intestinal lymphatic trunks for 10 min at 1 h, 2 h, and 3 h after OFL, according to the modified method described by Bollman et al. (22). In order to ascertain whether the samples were properly collected from the intestine, the lymph from three different origins, the hepatic lymphatic trunk, thoracic duct, and intestinal lymphatic trunk, and plasma from the inferior vena cava as a control were drained. One microliter of sample was subjected to SDS-PAGE and transferred onto the membrane, which was blocked by Blocking One (Nacalai Tesque, Kyoto, Japan). The membrane was incubated with anti-mouse apoB antibody and anti-rabbit IgG antibody, followed by detection with the ECL

Advance Detection Kit. The concentrations of TG, FFA, and glycerol in the intestinal lymph were measured at each point of time after OFL.

At 3 h after OFL, 10 μl of intestinal lymph was diluted with saline up to 100 μl and loaded into the HPLC columns, followed by the simultaneous and continuous detection of TC, TG, and PL. The flow-through was subfractioned into 84 tubes for 15 s each, 150 μl per tube. Samples (100 μl) were taken from each of subfraction tubes 16 to 25, which contained CM remnant-sized fractions of intestinal lymph, mixed together, and loaded into the tube of a centrifugal concentrator (Centricon Y-10, Amicon Millipore Corp., Bedford, MA). Concentrated samples (50 μl) were immunoblotted with anti apoB antibody as previously described.

Purification of total RNA from intestinal epithelium, cDNA synthesis, and quantitative real time-PCR

The intestines of CD36-KO (n = 6) and WT (n = 6) mice were removed during fasting and 3 h after OFL, divided into three segments, and washed with PBS. Epithelial stratum was stripped with slide glasses, collected, and stored with the RNA stabilization reagent, RNAlater (QIAGEN GmbH, Hilden, Germany) at 4°C. After being homogenized with QIAzol lysis reagent, the total RNA contents of the duodenum were isolated using the RNeasy Lipid Tissue Mini Kit (cat. 70804, QIAGEN GmbH), followed by treatment with DNase I (Cat. 79254, QIAGEN). Total RNA was collected in 50 μl of RNase-free water and stored at −80°C. One microgram of total RNA was primed with 50 pmol of oligo (dT) 20 and reverse transcribed to cDNA using the SuperScript III First Strand Synthesis System for RT-PCR (200 U, cat.18080-051, Invitrogen Corp., Carlsbad, CA). DNA polymerase and SYBR Green I (cat.#F-410, Finnzymes Oy, Espoo, Finland) were used in a reaction volume of 20 μl using gene-specific primers (5 μM) on cDNA (corresponding to ~50 ng total RNA) by an DNA engine Opticon 2 real-time PCR detection system (Bio-Rad Laboratories, Hercules, CA) (23). The $2^{-\Delta\Delta CT}$ method of relative gene expression was employed and a standard deviation of ct value of <0.3 was accepted. Results were expressed as arbitrary units in comparison with the expression of GAPDH.

Primers for this study

The sequence data of the genes was found with GenBank and the sequences of primers were designed with Primer3 (http://frodo.wi.mit.edu/cgi-bin/primer3/primer3_www.cgi). GAPDH was used as a housekeeping gene. The sequence and information for primers used in this study are as follows: mouse FAS (GenBank accession number; NM 007988): 5′-gctgcggaaacttcaggaaat-3′ and 5′-agagacgtgtcactcctggactt-3′, mouse acetyl-CoA carboxylase-1 (NM 133360): 5′-gaatcctcattggcttacgatgag-3′ and 5′-caatggcccggcatgt-3′, mouse stearoyl-CoA desaturase 1 (NM 009127): 5′- cctttcccttcgactactctg-3′ and 5′′-gccatgcagtcgatgaagaa-3′, mouse FABP1 (NM 017399): 5′-catccagaaagggaaggaca-3′ and 5′-ttttccccagtcatggtctc-3′, mouse FABP2 (NM 007980): 5′-ttgctgtccgagaggtttct-3′ and 5′-gctttgacaaggctggagac-3′, mouse FABP6 (NM 008375): 5′-caccattggcaaagaatgtg-3′ and 5′-caagccagcctcttgcttac-3′, mouse apoB (NM 009693): 5′-tgggattccatctgccatctcgag-3′ and 5′-gtagagatccatcacaggacaatg-3′, mouse Sar1b (NM 025535): 5′-ccgggaaaacaacttttgcta-3′ and 5′-atggtctgcacaatccacaa-3′, mouse MTTP (NM 008642: 5′-catgtcagccatcctgtttg-3′ and 5′-ctcgcgataccacagactga-3′, and mouse GAPDH (NM 008084): 5′-actccactcacggcaaattc-3′ and 5′-tctccatggtggtgaagaca-3′.

Statistical analysis

Data were shown as mean ± SD. Differences between the groups were evaluated using Student's *t*-test, and $P < 0.05$ was considered statistically significant.

RESULTS

Components of the MetS were clustered in patients with CD36-D

To investigate whether patients with CD36-D have phenotypes similar to those of subjects with MetS, we compared the clinical characteristics of CD36-D patients (n = 40) to those of age-, sex- and BMI-matched CD36-positive healthy volunteers (n = 84) in the fasting state. As shown in **Table 1**, during fasting, higher plasma levels of TG and glucose, lower levels of HDL-cholesterol, and higher systolic blood pressures were observed in the CD36-D patients compared with the controls. However, the plasma levels of TC, HbA1c, and adiponectin were not significantly changed. The number of risk factor components of MetS was greater in patients compared with controls (CD36-D patients vs. controls: 1.20 ± 0.80 vs. 0.76 ± 0.72, $P < 0.005$), and the percentage of the concurrence of more than one risk component of MetS was significantly higher in the patients [12/40 cases (30.0%) vs. 8/84 cases (9.5%), $P < 0.01$].

Concentrations of TG, apoB-48, FFAs, and Reml-C were elevated after OFL in patients with CD36-D

We previously reported that the plasma levels of TG and apoB-48 but not TC were higher in patients with CD36-D in the fasting state and postprandial state than in normal healthy subjects (9). In the current study, postprandial plasma lipid profiles were evaluated by loading OFTT cream after overnight fasting in patients with CD36-D and age-, sex- and BMI- matched control volunteers. The fasting levels of serum TG and apoB-48 and their postprandial changes (iAUC-TG and iAUC-ApoB48) were significantly increased in the patients compared with the control subjects. Furthermore, the peak points of TG and apoB-48 after OFL were delayed in the patients (**Fig. 1A**), which was consistent with the previous study (9). For the simultaneous evaluation of remnants in the course of the OFL study, Reml-C levels were also measured. Fasting plasma levels of Reml-C and its postprandial change (iAUC-Reml-C) were significantly enhanced in the patients. The

TABLE 1. Metabolic phenotypes of patients with CD36-D[a]

	CD36-D (n = 40)	Controls (n = 84)
Age (years)	62 ± 14	60 ± 7
Sex (male, female)	(25, 15)	(63, 21)
BMI (kg/m^2)	23.5 ± 3.6	23.5 ± 2
Total cholesterol (mg/dl)	201 ± 39	205 ± 32
TG (mg/dl)	178 ± 89[b]	126 ± 62
HDL-cholesterol (mg/dl)	46 ± 15[b]	61 ± 11
FPG (mg/dl)	110 ± 22[b]	95 ± 18
HbA1c (%)	6 ± 1.1	5.5 ± 1.3
Adiponectin (μg/ml)	5.9 ± 3.0[c]	7.2 ± 2.9[d]
Systolic BP (mmHg)	135 ± 18[b]	115 ± 15
Diastolic BP (mmHg)	80 ± 10	77 ± 18

CD36-D, CD36 deficiency; TC, total cholesterol.
[a] Values are the mean ± SD.
[b] $P < 0.01$.
[c] n = 5.
[d] n = 12.

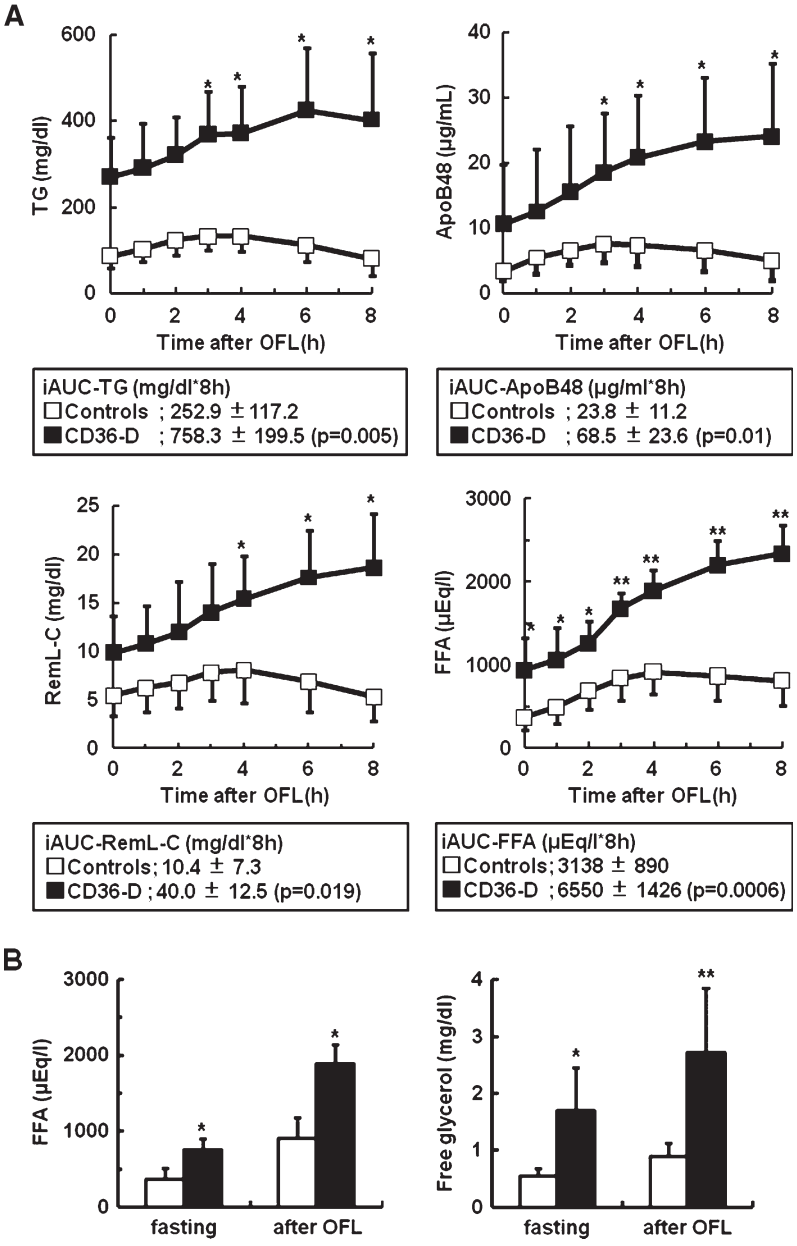

Fig. 1. The oral fat loading (OFL) test in patients with CD36 deficiency (CD36-D). Patients with CD36-D (n = 4, closed squares) and healthy controls matched for age, sex, and body weight (n = 12, open squares) were loaded with OFTT cream (containing 35% fat without sugar, 30 g fat/m^2 body surface area) after overnight fasting. Blood was drawn during fasting and 1, 2, 3, 4, 6, and 8 h after OFL, and serum and plasma were separated immediately. A: Triglyceride (TG), apolipoprotein B-48 (apoB-48), and Reml-C levels were measured, and the incremental area under the curve (iAUC) of each of these parameters was calculated. * $P < 0.05$ vs. controls. B: Free fatty acid (FFA) levels were measured at indicated times, and free glycerol levels were determined during fasting and 4 h after OFL. * $P < 0.05$, ** $P < 0.0005$ vs. controls. All values are the mean ± SD.

peak point of Reml-C was delayed more than 6 h in the patients, in accordance with the postprandial patterns of TG and apoB-48 (Fig. 1A). On the contrary, plasma levels of other apolipoproteins (apoAI, AII, B-100, CII, CIII, and E) were not significantly changed after OFL (data not shown), suggesting that the assembly of VLDL and HDL in the liver was not influenced by OFL. The further increase of Reml-C after OFL might be due to increases in CM remnant or VLDL remnants. Plasma CM remnants, but not VLDL remnants, were expected to increase in the patients because plasma apoB-48 levels increased remarkably in the patients and there was no change in the postprandial levels of other lipoproteins containing apoB-100 (data not shown). Plasma concentrations of FFA and free glycerol were significantly higher in the patients not only during fasting but after OFL than those of the controls (2-fold higher in CD36-D patients during fasting and after OFL) (Fig. 1B). These increases in TG, apoB-48, Reml-C, FFAs, and free glycerol after OFL might be the result of either overproduction or decreased clearance of CM and CM remnants from the intestines (Fig. 1A and B).

HPLC analysis of plasma lipoproteins after OFL in CD36-D patients

In our previous studies, the midband in polyacrylamide gel electrophoresis was observed and intermediate density lipoprotein cholesterol was increased in the fasting state in CD36-D patients compared with controls (9). For the analysis of postprandial lipoprotein profile in patients with CD36-D, HPLC analysis of plasma was performed during fasting and 4 h after OFL (**Fig. 2A**). Chromatographic patterns of TG in fasting state analysis showed that peaks of

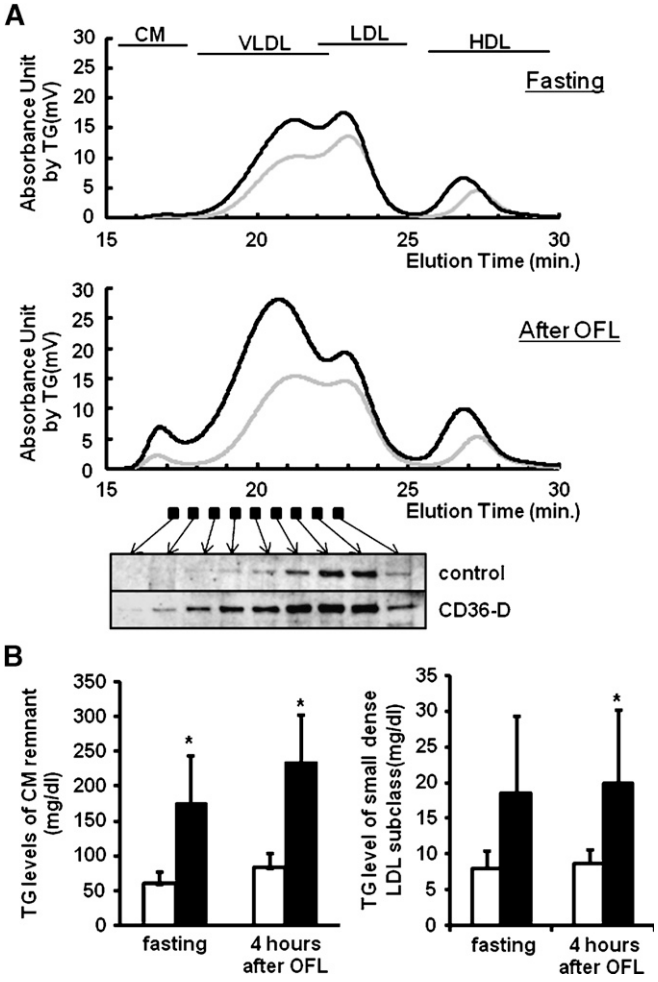

Fig. 2. Analysis of fasting and postprandial lipoprotein profiles by an HPLC method and Western blotting. Two hundred microliters of plasma were loaded into TSK gel Lipopropak XL columns. The concentrations of total cholesterol (TC) and triglyceride (TG) in the flow-through were measured continuously and simultaneously both during fasting and 4 h after oral fat loading (OFL). A: Representative chromatographic patterns of TG during fasting and at 4 h after OFL in patients (black line) and controls (gray line) are shown. Postprandial plasma was subfractionated into 84 tubes by HPLC, and 15 μl of flow-through was taken from each tube, which was expected to contain chylomicron (CM) remnants. ApoB-48 proteins were detected in samples from the controls (upper) and patients (lower) by anti-human apoB-48 antibody. B: TG concentrations in fractions of CM remnants and small dense LDL (sdLDL) during fasting and after OFL. TG concentrations of CM remnants and sdlDL fractions were calculated by the area under the chromatographic patterns by the detection of TG at fasting and 4 h after OFL. * $P < 0.01$ vs. controls. All values are the mean ± SD. CD36-D, closed squares; controls, open squares.

VLDL-sized and LDL-sized fractions were higher in patients (black line) compared with controls (gray line) (TG concentration in the VLDL-sized fraction: 128.5 ± 72.3 vs. 60.9 ± 16.6 mg/dl, $P = 0.037$; LDL: 50.9 ± 29.0 vs. 29.3 ± 8.8 mg/dl, $P = 0.03$). After OFL, the peak of CM was enhanced further in the patients compared with controls (TG concentration in the CM fraction: 18.2 ± 9.8 vs. 3.7 ± 2.4 mg/dl, $P = 0.04$). The TG levels of VLDL-sized and LDL-sized fractions were increased more, and the new peak (elution time: 20.8 minutes) was observed in the patients (TG concentration in the VLDL-sized fraction: 212.6 ± 62.7 vs. 83.3 ± 20.7 mg/dl, $P = 0.037$; LDL-sized fraction: 63.1 ± 23.5 vs. 30.0 ± 8.3 mg/dl, $P = 0.06$) (Fig. 2A). In the controls, apoB-48 protein was detected in the narrow range between the VLDL-sized and the LDL-sized fractions, while in the patients, apoB-48 was detected in the wide range (in all lanes) (Fig. 2A). The apo-B48 mass was huge in the new peak in VLDL-sized fractions. The TG concentrations of apoB-48–containing fractions (elution time: 19–22 min) were higher during fasting in the patients ($P = 0.019$) and in the postprandial state ($P = 0.010$) compared with the controls (Fig. 2B).

The change in the sdlDL subclass after OFL was also evaluated. The cholesterol levels of the sdlDL subclass did not significantly change either during fasting (35.1 ± 6.2 vs. 42.4 ± 13.2 mg/dl, $P = 0.17$) or after OFL (35.3 ± 4.7 vs. 41.4 ± 13.9 mg/dl, $P = 0.11$). However, the peak of LDL was moved to the right, with smaller LDL-sized fractions in the patients after OFL (elution time: 23.27 ± 0.08 vs. 23.15 ± 0.14 min, $P = 0.03$), while there was no difference in the fasting state (elution time: 23.13 ± 0.18 vs. 23.14 ± 0.13 min, $P = 0.46$), suggesting that the sdlDL particle might be increased after OFL in the patients. Furthermore, TG levels of the sdlDL subclass were higher during fasting and increased after OFL in CD36-D patients compared with controls (Fig. 2B).

Postprandial increase of plasma TG levels in CD36-KO mice, not associated with LPL activity

Figure 3A shows the result of the OFL test in CD36-KO (n = 8) and WT (n = 8) mice loaded with 17 μl/g BW of olive oil by gavage. During the fasting state, plasma TG levels were significantly higher in CD36-KO mice compared with WT mice (CD36-KO vs. WT mice; 51 ± 6 vs. 91 ± 30 mg/dl, $P = 0.010$). Two peaks of plasma TG levels (2-fold higher at 3 h and 6 h after OFL) were observed in CD36-KO mice, similar to the pattern in the OFL test in patients with CD36-D. Postprandial plasma lipoprotein profiles were analyzed by HPLC in both CD36-KO and WT mice. Fasting TG contents of the VLDL-sized fraction were higher in CD36-KO mice compared with WT mice (VLDL: 93.8 ± 30.8 vs. 66.7 ± 20.1 mg/dl, $P = 0.05$), while there was no difference in the LDL-sized fraction (LDL: 17.4 ± 2.5 vs. 17.6 ± 3.9 mg/dl, $P = 0.46$). After OFL, the TG contents of CM, VLDL, and LDL in CD36-KO mice were much higher compared with WT as well (CM: 110.9 ± 46.0 vs. 11.0 ± 8.3 mg/dl, $P = 0.005$; VLDL: 236.6 ± 51.8 vs. 77.1 ± 18.6 mg/dl, $P = 0.012$; LDL: 44.0 ± 10.2 vs. 22.3 ± 2.4 mg/dl, $P = 0.006$). The peak of the VLDL-sized fraction was higher and shifted toward larger particle size, as observed in patients after OFL. Furthermore, plasma levels of FFA and free glycerol were markedly increased in CD36-KO mice after OFL (Fig. 3B).

The secretion of CM from the intestine and VLDL from the liver in CD36-KO mice was examined with lipoprotein lipolysis blocked by the LPL inhibitor triton WR-1339 (Fig. 3C). After overnight fasting, CD36-KO and WT mice

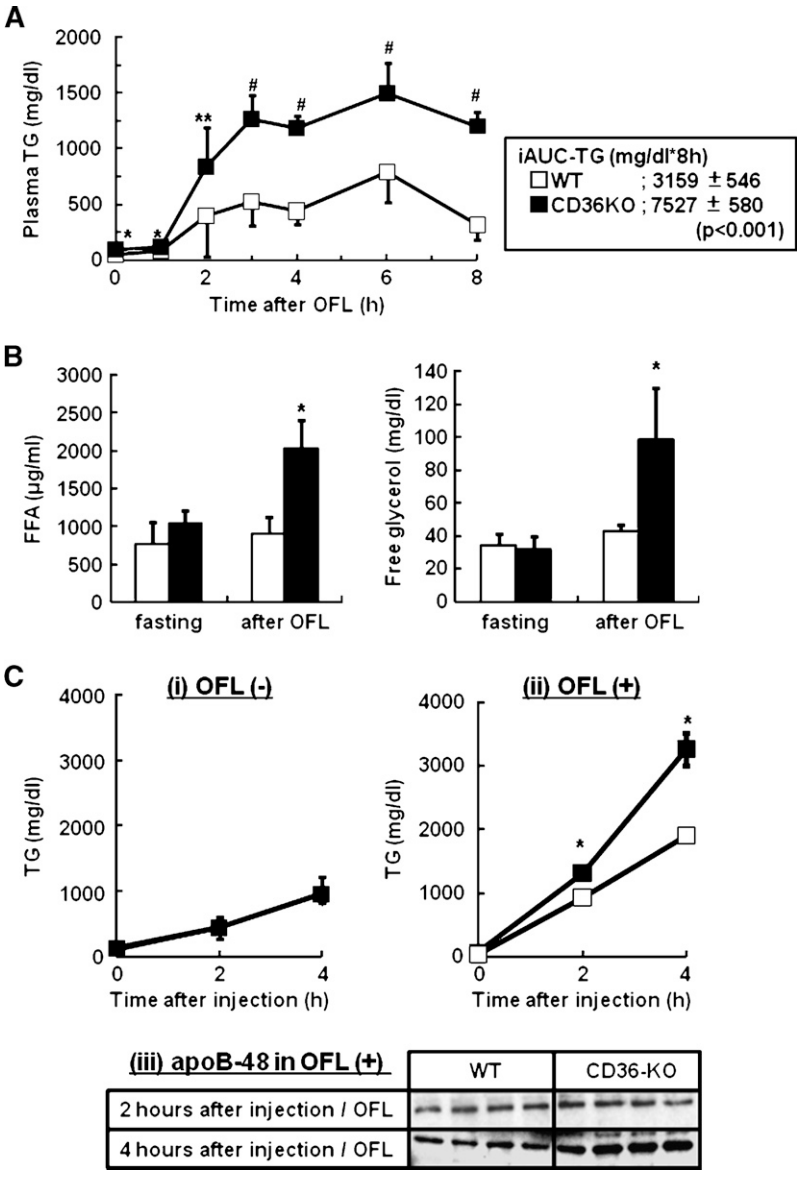

Fig. 3. OFL test in wild-type (WT) and CD36-KO mice CD36-KO and WT (C57BL6/J) mice, which were male and 8–12 weeks of age, with body weights of 18–24 g, were prepared after overnight fasting (more than 16 h). A: The OFL of mice using olive oil (17 μl/g body weight). TG levels of CD36-KO (n = 9) and WT (n = 8) mice were measured before and 1, 2, 3, 4, 6, and 8 h after OFL. * $P < 0.05$, ** $P < 0.01$, # $P < 0.001$ vs. WT mice. B: Postprandial changes of FFAs and free glycerol in mice. FFA and free glycerol levels of CD36-KO (n = 6) and WT (n = 6) mice were measured during fasting and 3 h after OFL. * $P < 0.05$ vs. WT mice. C: Triton WR-1339 experiments with and without OFL. After overnight fasting, two groups of CD36-KO (n = 6) and WT (n = 6) mice were injected with triton WR-1339 (500 mg/kg) intravenously. (i) OFL (−) experiment: after the injection, TG levels were measured at 0, 2, and 4 h without OFL. (ii) OFL (+) experiment: mice were loaded with 17 μl olive oil/g body weight within a few minutes after the injection of triton WR-1339, TG levels were measured at 0, 2, and 4 h after OFL. (iii) ApoB-48 mass of OFL (+) experiment. The apoB-mass of plasma samples at 2 and 4 h after OFL was compared between CD36-KO (n = 4) and WT (n = 4) mice. The same dose of plasma samples (1 μl of plasma diluted by PBS) was subjected to SDS-PAGE, and apoB-48 proteins were detected using anti-mouse apoB-48/B-100 antibody. Values are the mean ± SD.

were injected with triton WR-1339 in the fasting state. Plasma TG levels were increased after injection, but there was no difference between them. These results suggested that there might be no difference in the hepatic production of VLDL between CD36-KO and WT mice. On the contrary, we performed OFL in WT and CD36-KO mice after the injection of triton WR-1339. Plasma TG levels were remarkably higher in CD36-KO mice compared with WT mice, along with the increase of apoB-48 (Fig. 3C). The postprandial TG increase in CD36-KO mice might be caused by the increase of lipoprotein production (CM or CM remnants) from the intestine. This possibility was supported by the increase of plasma apoB-48 mass after OFL in CD36-KO mice. Furthermore, there was no significant difference in LPL and HL activity between CD36-KO mice and WT mice (LPL activity: 126 ± 65 vs. 135 ± 28 nmol FFA/ml/min, $P = 0.41$; HL activity; 72 ± 20 vs. 76 ± 16 nmol FFA/ml/min, $P = 0.38$). These data supported the hypothesis that lipoprotein synthesis in the small intestine was enhanced in CD36-KO mice, compared with WT mice after OFL.

Histological analysis of postprandial lipid absorption in CD36-KO mice

In order to histologically evaluate the dynamic change of intestinal lipid contents during fasting and after OFL, the small intestines of CD36-KO mice were stained with Oil Red O (**Fig. 4A–F**) and studied by electron microscopy (Fig. 4G–J) in the fasting state and after OFL. In the earlier histological assessment of the small intestines in CD36-KO mice by Drover et al. (13), they showed that the intestinal epithelium in CD36-KO mice fed a high-fat, high-carbohydrate diet ad libitum was rich in oil droplets. They also showed that the intestinal lipid contents were increased in CD36-KO mice after a long spell on a Western diet. In the present study, we investigated the short-term lipid movement

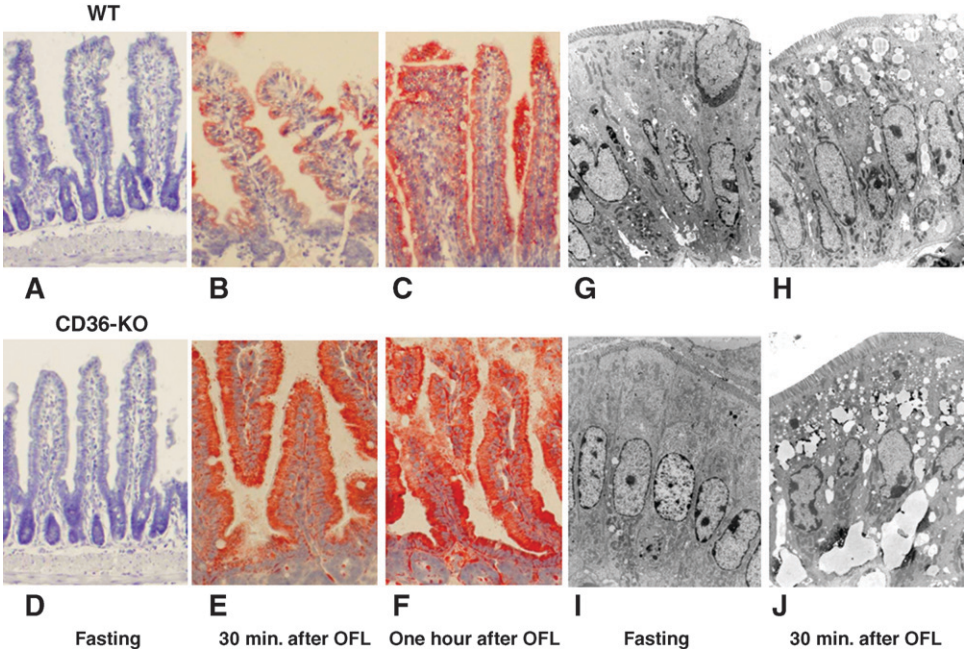

Fig. 4. Histological study of mouse intestine during fasting and after OFL. Fasting and postprandial lipid contents of the intestinal epitherium were compared. CD36-KO and WT mice were fed a normal chow diet and fasted overnight. A–F: Oil Red O and hematoxylin staining. Three groups of mice (CD36-KO, n = 4, WT, n = 4) were prepared, matched by age and body weight. The animals were anesthetized and the small intestines were removed during fasting in the first group, 30 min after OFL in the second group, and 1 h after OFL in the third group. The intestines were divided into three parts, after which the oral part was washed with PBS, fixed with 4% paraformaldehyde, and incubated with 30% sucrose overnight at 4°C. Intestinal samples were cryoembedded in Tissue-TeK O.C.T. compound and applied to slides after the subsequent cryostat sectioning, followed by staining with Oil Red O and hematoxylin. Intestines of WT mice during fasting (A), at 30 min after OFL (B), and at 1 h after OFL (C). CD36-KO mice during fasting (D), at 30 min after OFL (E), and at 1 h after OFL (F). G–J: Electron microscopic analysis. Two groups of mice (CD36-KO, n = 4, WT, n = 4) were prepared, matched by age and body weight. The first group of mice (CD36-KO mice, n = 4 and WT mice, n = 4) was anesthetized in the fasting state and their intestines are fixed by the intraventricular injection of 2% glutaraldehyde; the second group was treated in the same way 30 min after OFL. The small intestines were removed for sections in the same position as in the Oil Red O study. The intestines were fixed with 1% osmium tetroxide and stained by the uranyl acetate. Ultrathin sections were analyzed using a Hitachi H-7100 electron microscope. Intestines of WT mice during fasting (G), at 30 min after OFL (H); intestines of CD36-KO mice during fasting (I) and at 30 min after OFL (J).

in the intestinal epithelium after OFL in CD36-KO mice. During fasting, almost no deformity and no lipid droplets were observed in the intestine along the gastro-colic and crypt-to-villus axes in both groups (Fig. 4A, D). After OFL, numerous lipid droplets were observed in the intestinal epithelium of CD36-KO more than WT mice during the early stage of the OFL (Fig. 4B, E), and the lipid droplets moved to the vasolateral side (Fig. 4C, F). In the electron microscopic study, there was no apparent difference in the structure and number of lipid droplets in the fasting state (Fig. 4G, I). After OFL, the number of lipid droplets was markedly increased in the vasolateral side of the intestinal epithelium of CD36-KO mice compared with WT mice (Fig. 4H, J). These data suggest that production of lipids is faster and increased in the small intestine in CD36-KO mice.

Lipoprotein secretion into the intestinal lymph in CD36-KO mice

After OFL, the intestinal lymphatic trunks in CD36-KO (n = 4) and WT mice (n = 4) were cannulated as described in Materials and Methods. As shown in **Fig. 5A**, only apoB-48, but not apoB-100, was present in the collected lymph from the intestinal lymphatic trunks. Thus, lipoproteins derived from the intestine (contained in the intestinal lymph) could be either CM or HDL but not apoB-100–containing lipoproteins (VLDL, intermediate density lipoprotein, or LDL). In our study, the intestinal lymphatic fluid was collected into tubes for only 10 min, not by the continuous cannulation of tubes in the intestinal lymphatic trunks as performed in other studies (12, 13), to protect the small intestine from surgical invasion and malfunction of lipid absorption. The TG levels of the intestinal lymph in CD36-KO mice were significantly increased at 3 h after OFL compared with WT mice (Fig. 5B).

Postprandial HPLC chromatographic patterns of the intestinal lymph were compared by the detection of TG and PL between CD36-KO (n = 4) and WT (n = 4) mice, and representative patterns of both groups of mice are shown in Fig. 5C. There was no remarkable change in TG and PL patterns between the two groups in the fasting state (data

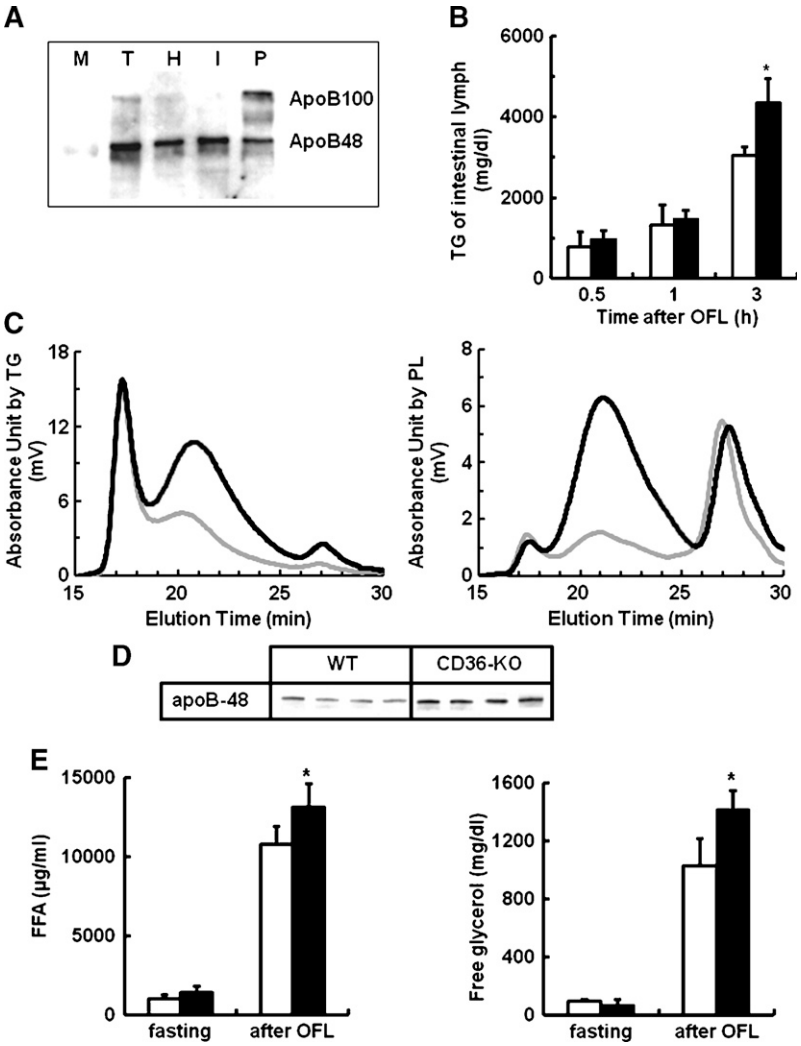

Fig. 5. Lipoprotein analysis of mouse intestinal lymph after OFL. Intestinal lymph was collected during fasting and after OFL using the modified method of Bollman, Cain, and Grinlay (22). A: Identification of the intestinal lymph. Lymph was drained from three different trunks, the hepatic lymphatic trunk (lane H), thoracic duct (lane T), and intestinal lymphatic trunk (lane I). Lymph fluids were collected in the same amount, diluted with PBS, and loaded onto SDS-PAGE along with plasma in the same amount as a positive control (lane P). ApoB-48 and apoB-100 protein were detected using anti-mouse apoB-48/B-100 antibody. During fasting and at 30 min and 2 and 3 h after OFL, CD36-KO (n = 5) and WT (n = 5) mice were anesthetized, and intestinal lymph was collected for 10 min from the intestinal lymphatic trunk. B: TG levels of the intestinal lymph after OFL. TG levels of the intestinal lymph were measured at the indicated time by the enzymatic method. *$P < 0.001$, vs. WT. Ten microliters of the intestinal lymph at 3 h after OFL were subjected to an HPLC column. TG and phospholipids (PL) concentrations of the flow-through were continuously measured. C: Representative chromatographic patterns of the intestinal lymph. By the detection of TG and PL at 3 h after OFL, HPLC patterns were shown in CD36-KO (solid line) and WT (gray line) mice. D: The apoB-48 mass of CM remnant-sized fractions. CM remnant-sized fractions were deduced to be present by the detection of apoB within the flow-through of mouse intestinal lymph. The flow-through of these fractions was concentrated and subjected to SDS-PAGE (WT mice, n = 4, CD36-KO mice, n = 4), and apoB-48 proteins were detected using anti-mouse apo B-48/B-100 antibody. E: Postprandial changes of FFA and free glycerol levels of the intestinal lymph. Concentrations of FFA and free glycerol were measured by the enzymatic method in CD36-KO (n = 4, closed squares) and WT (n = 4, open squares) during fasting and 3 h after OFL. * $P <$ 0.05 vs. WT. Values are the mean ± SD.

not shown). At 3 h after OFL, three peaks were observed in the HPLC patterns by the detection of TG, located in the CM-sized, VLDL-sized, and HDL-sized fractions. ApoB-100 was not present in the intestinal lymph (Fig. 5A), suggesting that peak of lipoproteins in VLDL-sized fractions might be intestine-derived lipoproteins smaller than CM in size, but not VLDL or LDL, since we compared the fraction range of these lipoproteins with those of human plasma lipoproteins (Fig. 2A). The TG contents of these lipoprotein fractions were remarkably higher in CD36-KO compared with WT mice (362.2 ± 34.6 vs. 254.7 ± 28.4, $P = 0.0017$), with the higher peak (elution time: 20.5 min) corresponding to the peak of CM remnants in the patients with CD36-D (Fig. 2A). Furthermore, the PL contents of these fractions were significantly higher in CD36-D mice compared with WT mice (115.9 ± 16.9 vs. 42.2 ± 4.8 mg/dl, $P = 0.001$), along with the higher ratio of PL/TG (0.322 ± 0.052 vs. 0.166 ± 0.019, $P = 0.005$) (Fig. 5C). The apoB-48 mass of these lipoproteins of CD36-KO was also higher than that of WT mice (Fig. 5D). Lipoproteins smaller than CM in size produced in the intestinal lymph was significantly enhanced in CD36-KO mice, along with increases of TG and PL contents, compared with WT mice. FFA and free glycerol levels secreted in the intestinal lymph at 3 h after OFL were also higher in CD36-KO mice compared with WT mice (Fig. 5E), while there was no difference in the fasting state.

MRNA levels of genes involved in the biosynthesis of FFA and the assembly of CM

The total mRNA of the epithelial intestinal cells of CD36-KO (n = 6) and WT mice (n = 6) during fasting and after OFL was isolated and transcribed to cDNA. Subsequently, the expression levels of mRNA of nine genes in the intestinal epithelial cells were evaluated (**Fig. 6**). The mRNA levels of FAS, an enzyme involved in the biosynthesis of FFA, were significantly higher in CD36-KO mice in the fasting state, and the increase of FAS mRNA levels continued during postprandial states compared with WT mice. The mRNA level of SCD1, a lipogenic enzyme in the biosynthesis of monounsaturated fatty acids [mainly oleate; (C18:1) and palmitoleate (C16:1)], was not different in the fasting state but increased significantly in CD36-KO mice in the postprandial state. On the other hand, there was no significant difference in acetyl-CoA carboxylase-1 (an enzyme that converts acetyl CoA to malonyl CoA) mRNA levels

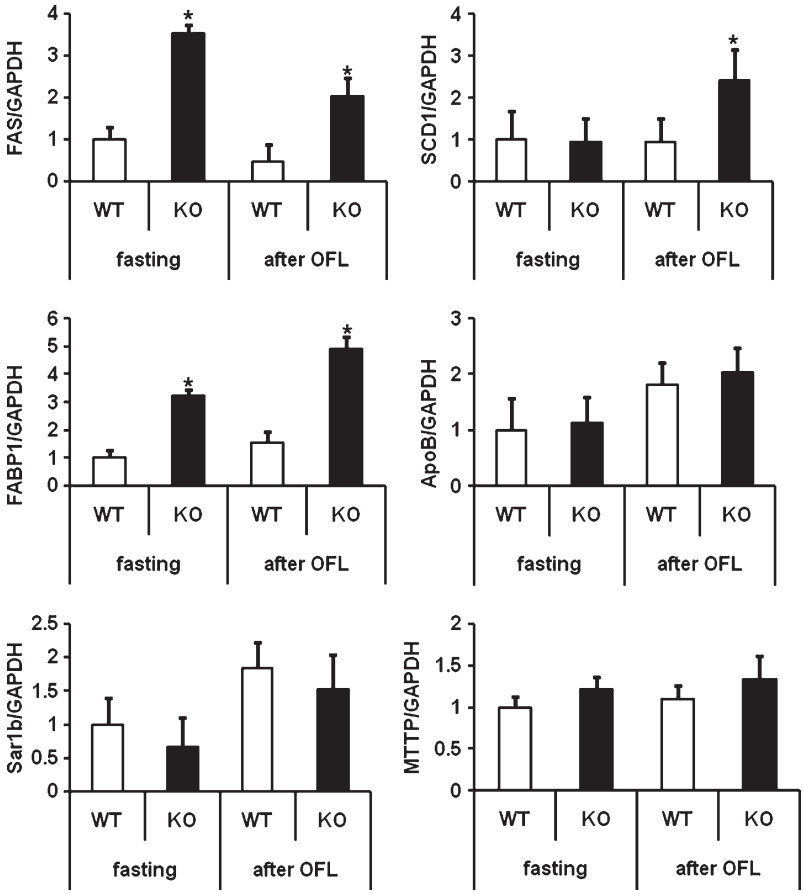

Fig. 6. Quantitative PCR of genes expressed in the intestinal epithelium The intestinal epithelia of CD36-KO (n = 6, closed square) and WT (n = 6, open square) mice during fasting and 3 h after OFL were stripped; total RNA was isolated and transcribed to cDNA; and the mRNA levels of genes were evaluated by real-time quantitative PCR, as described in Materials and Methods. The relative abundances of genes were calculated by comparison with mRNA levels of GAPDH. * $P < 0.05$ vs. WT. Values are the mean ± SD.

between them. Among other families of FABPs, FABP-1 is abundantly expressed in the small intestine. The mRNA level of FABP-1 was higher during fasting and increased more after OFL in CD36-KO mice. There was no significant difference in the mRNA levels of apoB and microsomal TG transfer proteins between CD36-KO and WT mice both in the fasting state and after OFL. The mRNA expression of Sar1b, which is the gene responsible for CM-retention disease, was relatively lower in CD36-KO mice compared with WT mice, but the difference was not statistically significant.

DISCUSSION

In the present study, we clarified that *1*) metabolic disorders in CD36-D were independent of visceral fat accumulation and CM remnants were increased in patients in the postprandial state along with an increase of sdlDL particles, *2*) the production of lipoprotein smaller than CM in size into the intestinal lymph was increased in CD36-KO mice along with high levels of FFA and free glycerol, and *3*) increase of lipoproteins smaller than CM in size might be associated with the increase of endogenous FA secretion from the intestine. These results suggested that the postprandial characteristics of lipoprotein metabolism in CD36-D might be related to their atherogenicity.

Metabolic disorders in CD36-D were independent of visceral fat accumulation and CM remnants were increased in patients in the postprandial state along with an increase of sdlDL particles

Although our earlier studies showed that metabolic disorders such as dyslipidemia, hypertension, and hyperglycemia are clustered in patients with CD36-D (9, 10), its underlying mechanism has not yet been clarified. Therefore, in the present study, we investigated the causes of clustered metabolic disorders, in particular, the cause of the postprandial hyperlipidemia in CD36-D. As shown in Table 1, we re-examined metabolic disorders in patients with CD36-D. The patients (n = 40) were not obese (BMI; 23.3 ± 2.9); their plasma adiponectin levels were not lower compared with the controls. Some participants in this study received an abdominal CT scanning test for the measurement of visceral fat area; there was no significant difference patients and the controls. Therefore, the metabolic phenotypes of CD36-D might be independent of visceral fat accumulation.

In our previous studies, two independent risk factors for atherosclerotic disease, insulin resistance and postprandial hypertriglyceridemia, were observed in CD36-D (9, 10). Insulin resistance and postprandial hypertriglyceridemia are influenced by the impaired catabolism of TRL (6). Moreover, the postprandial accumulation of TRL was associated with the development of atherosclerotic disease (24). Thus, we assumed that the metabolic disorders in patients with

CD36-D might be closely related to the impaired metabolism of TRL and RLP and independent of visceral fat accumulation. In the previous study, we found an accumulation of remnants in fasting serum of patients as a midband of polyacrylamide gel disc electrophoresis and high levels of intermediate density lipoprotein-cholesterol (10). We assessed the hypothesis that the impaired metabolism of TRL and remnants was one of the important causes of the metabolic disorders in patients with CD36-D. In this study, fasting levels and postprandial increases of Reml-C were significantly higher in patients with CD36-D (Fig. 1A). These changes were in parallel with those of TG and apoB-48, suggesting that the postprandial increases of Reml-C were due to the accumulation of CM remnants. We examined the HPLC patterns of plasma from the patients and the controls along with detecting apoB-48 proteins by Western blotting. An increased peak of lipoproteins in the size of VLDL was observed after OFL in CD36-D patients (Fig. 2A). ApoB-48 mass and TG contents of these lipoproteins were increased in the patients during fasting and in the postprandial state (Fig. 2A, B). However, the concentrations of apoB-100 did not change during fasting and after OFL; the increase of TG content in lipoproteins in size of VLDL was mainly due to the increase of intestine-derived lipoproteins (CM or CM remnants). FFAs and free glycerol levels, which are among the catabolized products from CM and CM remnants, were increased in patients after OFL (Fig. 1B). In the previous study, we measured the activity of HL and LPL and found there was no difference (10). However, in patients with CD36-D, decreased rates of CM clearance cannot be ruled out as this was not directly measured. Besides the increase of CM remnants, we found the increase of sdlDL particles, which is an independent risk factor of atherosclerosis (25). The genesis of sdlDL was suggested to be associated with the impaired postprandial clearance of TRL by enhancing the transfer of TG to LDL in conjunction with the reverse transfer of cholesteryl esters from HDL mediated by cholesteryl ester transfer protein and the subsequent hydrolysis of core TG to sdlDL by HL (26, 27).

Taken together, in patients with CD36-D, high levels of TG, apoB48, FFA, and free glycerol in the fasting state, postprandial increase of CM or CM remnants and the presence of sdlDL were observed. However, the metabolic abnormalities were not clearly distinguished whether the metabolic abnormalities were a primary effect due to CD36-D or were due to insulin resistance, which is accompanied by CD36-D.

The production of lipoproteins smaller than CM in size were increased in the small intestine

Previously, Drover et al. (13) and Goudriaan et al. (14) evaluated postprandial hypertriglyceridemia in CD36-KO mice. They confirmed by examinations in vitro and in vivo that the intestinal uptake of FFAs was not impaired in CD36-KO. Histologically, a large number of lipid droplets was observed in the intestinal epithelium of CD36-KO mice fed a high-fat diet ad libitum (13), and the recovery of [^{3}H] labeled TG loaded orally into the intestinal lymph was lower in CD36-KO mice compared with WT mice (14). They concluded that the postprandial increase of TG was due to the feedback inhibition of LPL by the high concentration of plasma FFA and apoC-III after OFL (13, 14). Their conclusions could explain one aspect of the mechanism of postprandial hyperlipidemia in CD36-KO mice.

In the current study, we focused on the production of lipoproteins from the intestine in CD36-KO mice compared with WT mice. TG levels were not different in both CD36-KO and WT mice after injection of triton WR-1339 in the fasting state, suggesting that there was no apparent difference in the production of VLDL by the liver (Fig. 2C). This result in the fasting state was consistent with those of Drover et al. (13) and Goudriaan et al. (14). The combination experiment of the OFL test and triton WR-1339 injection was also performed by them (13, 14). The purpose and the timepoint of OFL were different from what we performed; they injected triton WR-1339 after OFL and concluded that there is little additional inhibition when adding triton WR-1339 in CD36-KO mice. To the contrary, after we injected triton WR-1339 in the fasting state, we performed OFL for the purpose of adding lipid production from the small intestines. As a result, TG increase after OFL was significantly higher in CD36-KO mice compared with WT mice along with the increase of apoB-48 mass, which clearly suggests that the production of intestine-derived lipoproteins is accelerated in CD36-KO mice under condition of LPL inhibition by triton WR-1339. Drover et al. (13) pointed out that more lipid droplets were observed in the intestinal epithelium of CD36-KO mice fed a high-fat diet ad libitum, and supposed that these changes were due to an impaired movement of lipids into the intestinal lymph. To the contrary, we used fasted mice fed a normal diet avoiding the difference of elapsed time after feeding between individuals and found that more lipid droplets emerged in the epithelium of CD36-KO mice in the earlier stage after OFL (Fig. 4), which clearly suggested that intestine-derived lipoproteins were produced more abundantly and passed by significantly faster in CD36-KO mice compared with WT. Moreover, we collected the intestinal lymph from mice for only 10 min and found that TG levels of the intestinal lymph in CD36-KO mice were significantly higher after OFL compared with those in WT mice (Fig. 5B). HPLC analysis showed that the increase of TG was mainly due to an increase in lipoproteins smaller than CM in size along with the higher content of PLs (Fig. 5C). In the present study, the pattern of changes of TG levels in the intestinal lymph after OFL in CD36-KO mice was opposite to that reported by Drover et al. (13) and Goudriaan et al. (14). One reason for this discrepancy might be the difference of procedure. In this study, intestinal lymph was carefully collected with a less-invasive technique and drained for 10 min for protecting the small intestine from severe surgical invasion and malfunction of lipid absorption. The other researchers examined intestinal TG secretion by continuous drainage from the intestinal lymphatic trunks with continuous lipid infusion from duodenal fistula. They did not confirm whether the experiments might be performed without damaging the intestinal functions.

Drover et al. (13) and Goudriaan et al. (14) showed that, in the postprandial state, LPL activity was impaired in CD36-KO mice because of the negative feedback of a higher concentration of FFAs even though it was not impaired in the fasting state. To the contrary, we showed that the postprandial intestinal lymph in CD36-KO mice was rich in lipoproteins smaller than CM in size. The result that the activity of LPL and HL was not impaired does not necessarily imply a lack of effect on CM and CM remnant clearance. A contribution to the increase of TG and CM in CD36-KO mice after OFL on a background diet of chow, by delayed plasma clearance of CM and CM remnants, cannot be ruled out, as this was not measured in the present study. Our finding that the production of lipoproteins smaller in size was increased suggests one possible mechanism in the postprandial increase of TG in CD36-KO mice.

Increase of lipoproteins smaller than CM in size might be associated with the increase of endogenous FA secretion from the intestine

In CD36-KO mice, FFA and glycerol levels were increased after OFL (Fig. 3B). Furthermore, we found a higher concentration of intestine-derived FFAs and glycerol in the intestinal lymph of CD36-KO mice compared with that of WT (Fig. 5E). The results are also consistent with increased fatty acid absorption, which was not measured in this study. Since we already showed the increase of intestine-derived lipoproteins smaller than CM in size, we focused on the increased synthesis of FFAs and formation of lipoproteins smaller than CM in size. The mRNA levels of molecules involved in primary FFA biosynthesis (FAS, SCD1, and FABP1) were significantly higher in CD36-KO mice (Fig. 6). The distorted composition of FFAs because of the impaired uptake of LCFA without CD36 might stimulate the chronic biosynthesis of endogenous FFAs. This enhanced production of FFAs might induce the de novo lipogenesis of TG, resulting in the increased synthesis of intestine-derived lipoproteins. Haidari et al. (28) showed that the de novo synthesis of FA and apoB-48-containing lipoproteins in the intestine of fructose-fed hamsters was increased. Even though this result was observed in an animal model of insulin resistance model, it was suggested that the endogenous production of fatty acids might influence the apoB-48-containing lipoprotein secretion in the small intestine. Endogenous lipids were secreted mainly in the fasting state in the size of VLDL (29), and almost half of total lymphatic TG was derived from endogenously synthesized sources in the postprandial state (30). It is known that PL in CM particles originates from the intestinal epithelium (31); therefore high PL contents of lipoproteins smaller than CM in size indicate that these lipoproteins might be derived from the endogenous source. Drover et al. (13) and Goudriaan et al. (14) suggested that high plasma FFA levels might be caused by the prolonged and deteriorated lipolysis of TRL and their remnants in CD36-D; however we have suggested that the de novo synthesis of FFA in the intestine and the increased production of lipoproteins smaller than CM in size were one reason for the postprandial hypertriglyceridemia.

Our data demonstrated the phenotypic expression of higher FFA, TG, and TRL levels in CD36-D after OFL. Furthermore, CM remnant-sized lipoproteins were increased in CD36-D. One strain of spontaneously hypertensive rats lacks CD36 and shows metabolic phenotypes of insulin resistance and high FFA levels, which are ameliorated by the transgenic overexpression of CD36 (32). Relationships between high plasma FFA level and CD36 gene polymorphisms in Caucasians (33) and mutations in the Japanese (34) have also been reported. High levels of FFAs in plasma were demonstrated to accelerate insulin resistance and cardiovascular risk in many epidemiological studies (35, 36); high FFA levels in patients with CD36-D might be one of the risk factors for atherosclerosis. In the former studies, CD36-D has been assumed to be anti-atherogenic since the uptake of oxidized LDL was reduced in macrophages from patients with CD36-D (7) and CD36-KO mice (37). However, in our clinical experience, the patients suffered from atherosclerotic cardiovascular diseases more frequently and severely than controls did (unpublished observation). In the current study, the increase in remnants plasma FFA level and presence of sdlDL were observed in patients with CD36-D; these could be risk factors for atherosclerosis.

In conclusion, we demonstrated the postprandial increase of plasma CM remnants and the presence of sdlDL with enhanced TG synthesis in the small intestine in the CD36-D state. CD36 might play an important role in lipid metabolism for the proper uptake and production of FFAs (LCFA) in the intestines and for the subsequent production of large-sized CM and catabolism of remnants. The increase of TRLs and their remnants and the accumulation of FFA might be closely associated with the development of atherosclerosis in the CD36-deficient state.

We gratefully acknowledge Sekisui Medical Co. Ltd., Fuji Rebio Inc., and Kyowa Medex and Skylight Biotech Inc. for technical assistance.

REFERENCES

1. Wilson, P. W. F., R. B. D'Agostino, D. Levy, A. M. Belanger, H. Silbershatz, and W. B. Kannel. 1998. Prediction of coronary heart disease using risk factor categories. *Circulation.* **97:** 1837–1847.
2. Hokanson, J. E., and M. A. Austin. 1996. Plasma triglyceride level is a risk factor for cardiovascular disease independent of high-density lipoprotein cholesterol level: a meta-analysis of population based prospective studies. *J. Cardiovasc. Risk.* **3:** 213–219.
3. Zilversmit, D. B. 1979. Atherogenesis: a postprandial phenomenon. *Circulation.* **60:** 473–485.
4. Havel, R. J. 1994. Postprandial hyperlipidemia and remnant lipoproteins. *Curr. Opin. Lipidol.* **5:** 102–119.
5. Cohn, J. S., C. Marcoux, and J. Davignon. 1995. Detection, quantification, and characterization of potentially atherogenic triglyceride-rich remnant lipoproteins. *Arterioscler. Thromb. Vasc. Biol.* **19:** 2474–2486.
6. Funada, J., M. Sekiya, T. Otani, K. Watanabe, M. Sato, and H. Akutsu. 2004. The close relationship between postprandial remnant metabolism and insulin resistance. *Atherosclerosis.* **172:** 151–154.
7. Yamashita, S., K. Hirano, T. Kuwasako, M. Janabi, Y. Toyama, M. Ishigami, and N. Sakai. 2007. Physiological and pathological roles

of a multi-ligand receptor CD36 in atherogenesis; insights from CD36-deficient patients. *Mol Cell Biochem.* **299:** 19–22.
8. Poirier, H., P. Degrace, I. Niot, A. Bernard, and P. Besnard. 1996. Localization and regulation of the putative membrane fatty-acid transporter (FAT) in the small intestine. *Eur. J. Biochem.* **238:** 368–373.
9. Miyaoka, K., T. Kuwasako, K. Hirano, S. Nozaki, S. Yamashita, and Y. Matsuzawa. 2001. CD36 deficiency is associated with insulin resistance. *Lancet.* **357:** 686–687.
10. Kuwasako, T., K. Hirano, N. Sakai, M. Ishigami, H. Hiraoka, M. J. Yakub, K. Yamauchi-Takihara, S. Yamashita, and Y. Matsuzawa. 2003. Lipoprotein abnormalities in human genetic CD36 deficiency associated with insulin resistance and abnormal fatty acid metabolism. *Diabetes Care.* **26:** 1647–1648.
11. Hajri, T., X. X. Han, A. Bonen, and N. A. Abumrad. 2002. Defective fatty acid uptake modulates insulin responsiveness and metabolic responses to diet in CD36-null mice. *J. Clin. Invest.* **109:** 1381–1389.
12. Febbraio, M., N. A. Abumrad, D. P. Hajjar, K. Sharma, W. Cheng, S. F. Pearce, and R. L. Silverstein. 1999. A null mutation in murine CD36 reveals an important role in fatty acid and lipoprotein metabolism. *J. Biol. Chem.* **274:** 19055–19062.
13. Drover, V. A., M. Ajmal, F. Nassir, N. O. Davidson, A. M. Nauli, D. Sahoo, P. Tso, and N. A. Abumrad. 2005. CD36 deficiency impairs intestinal lipid secretion and clearance of chylomicrons from the blood. *J. Clin. Invest.* **115:** 1290–1297.
14. Goudriaan, J. R., M. A. den Boer, P. C. Rensen, M. Febbraio, F. Kuipers, J. A. Romijn, L. M. Havekes, and P. J. Voshol. 2005. CD36 deficiency in mice impairs lipoprotein lipase-mediated triglyceride clearance. *J. Lipid Res.* **46:** 2175–2181.
15. The Committee for Japanese Definition of Metabolic Syndrome. 2005. Metabolic syndrome - definition and diagnostic criteria in Japan [n Japanese]. *J Jpn Soc Int Med.* **94:** 794–203.
16. Sakai, N., Y. Uchida, K. Ohashi, T. Hibuse, Y. Saika, Y. Tomari, S. Kihara, H. Hiraoka, T. Nakamura, S. Ito, et al. 2003. Measurement of fasting serum apoB-48 levels in normolipidemic and hyperlipidemic subjects by ELISA. *J. Lipid Res.* **44:** 1256–1262.
17. Miyauchi, K., N. Kayahara, M. Ishigami, H. Kuwata, H. Mori, H. Sugiuchi, T. Irie, A. Tanaka, S. Yamashita, and T. Yamamura. 2007. Development of a homogeneous assay to measure remnant lipoprotein cholesterol. *Clin. Chem.* **53:** 2128–2135.
18. Usui, S., Y. Hara, S. Hosaki, and M. Okazaki. 2002. A new on-line dual enzymatic method for simultaneous quantification of cholesterol and triglycerides in lipoproteins by HPLC. *J. Lipid Res.* **43:** 805–814.
19. Okazaki, M., S. Usui, A. Fukui, I. Kubota, and H. Tomoike. 2006. Component analysis of HPLC profiles of unique lipoprotein subclass cholesterols for detection of coronary artery disease. *Clin. Chem.* **52:** 2049–2053.
20. Moore, K. J., J. El Khoury J, L. A. Medeiros, K. Terada, C. Geula, A. D. Luster, and M. W. Freeman. 2002. A CD36-initiated signaling cascade mediates inflammatory effects of beta-amyloid. *J. Biol. Chem.* **277:** 47373–47379.
21. Lutz, E. P., M. Merkel, Y. Kako, K. Melford, H. Radner, J. L. Breslow, A. Bensadoun, and I. J. Goldberg. 2001. Heparin-binding defective lipoprotein lipase is unstable and causes abnormalities in lipid delivery to tissues. *J. Clin. Invest.* **107:** 1183–1192.
22. Bollman, J. L., J. C. Cain, and J. H. Grindlay. 1949. Techniques for the collection of lymph from the liver, small intestine, or thoracic duct of the rat. *J. Lab. Clin. Med.* **33:** 1349–1352.
23. Nishida, Y., K. Hirano, K. Tsukamoto, M. Nagano, C. Ikegami, K. Roomp, M. Ishihara, N. Sakane, Z. Zhang, K. Tsujii, et al. 2002. Expression and functional analyses of novel mutations of ATP-binding cassette transporter-1 in Japanese patients with high-density lipoprotein deficiency. *Biochem. Biophys. Res. Commun.* **290:** 713–721.
24. Karpe, F. 1999. Postprandial lipoprotein metabolism and atherosclerosis. *J. Intern. Med.* **246:** 341–355.
25. Krauss, R. M. 1991. Low density lipoprotein subclass and risk of coronary disease. *Curr. Opin. Lipidol.* **4:** 248–252.
26. Syvänne, M., and M. R. Taskinen. 1997. Lipids and lipoproteins as coronary risk factors in non-insulin-dependent diabetes mellitus. *Lancet.* **350:** 20–23.
27. Lemieux, I., C. Couillard, A. Pascot, N. Bergeron, D. Prud'homme, J. Bergeron, A. Tremblay, C. Bouchard, P. Mauriege, and J. P. Després. 2000. The small dense LDL phenotype as a correlate of postprandial lipemia in men. *Atherosclerosis.* **153:** 423–432.
28. Haidari, M., N. Leung, F. Mahbub, K. D. Uffelman, R. Kohen-Avramoglu, G. F. Lewis, and K. Adeli. 2002. Fasting and postprandial overproduction of intestinally derived lipoproteins in an animal model of insulin resistance. *J. Biol. Chem.* **277:** 31646–31655.
29. Ockner, R. K., F. B. Hughes, and K. J. Isselbacher. 1969. Very low density lipoproteins in intestinal lymph: origin, composition, and role in lipid transport in the fasting state. *J. Clin. Invest.* **48:** 2079–2088.
30. Shiau, Y. F., D. A. Popper, M. Reed, C. Umstetter, D. Capuzzi, and G. M. Levine. 1985. Intestinal triglycerides are derived from both endogenous and exogenous sources. *Am. J. Physiol. Gastrointest. Liver Physiol.* **248:** 164–169.
31. Luchoomun, J., and M. M. Hussain. 1999. Assembly and secretion of chylomicrons by differentiated caco-2 cells. *J. Biol. Chem.* **274:** 19565–19572.
32. Pravenec, M., V. Landa, V. Zidek, A. Musilova, V. Kren, L. Kazdova, T. J. Aitman, A. M. Glazier, A. Ibrahimi, N. A. Abumrad, et al. 2001. Transgenic rescue of defective CD36 ameliorates insulin resistance in spontaneously hypertensive rats. *Nat. Genet.* **27:** 156–158.
33. Ma, X., S. Bacci, W. Mlynarski, L. Gottardo, T. Soccio, C. Menzaghi, E. Iori, R. A. Lager, A. R. Shroff, E. V. Gervino, et al. 2004. A common haplotype at the CD36 locus is associated with high free fatty acid levels and increased cardiovascular risk in Caucasians. *Hum. Mol. Genet.* **13:** 2197–2205.
34. Kajihara, S., A. Hisatomi, Y. Ogawa, T. Yasutake, T. Yoshimura, T. Hara, T. Mizuta, I. Ozaki, N. Iwamoto, and K. Yamamoto. 2001. Association of the Pro90Ser CD36 mutation with elevated free fatty acid concentrations but not with insulin resistance syndrome in Japanese. *Clin. Chim. Acta.* **314:** 125–130.
35. Carlsson, M., Y. Wessman, P. Almgren, and L. Groop. 2000. High levels of nonesterified fatty acids are associated with increased familial risk of cardiovascular disease. *Arterioscler. Thromb. Vasc. Biol.* **20:** 1588–1594.
36. Pirro, M., P. Mauriege, A. Tchernof, B. Cantin, G. R. Dagenais, J. P. Despres, and B. Lamarche. 2002. Plasma free fatty acid levels and the risk of ischemic heart disease in men: prospective results from the Quebec Cardiovascular Study. *Atherosclerosis.* **160:** 377–384.
37. Febbraio, M., E. A. Podrez, J. D. Smith, D. P. Hajjar, S. L. Hazen, H. F. Hoff, K. Sharma, and R. L. Silverstein. 2000. Targeted disruption of the class B scavenger receptor CD36 protects against atherosclerotic lesion development in mice. *J. Clin. Invest.* **105:** 1049–1056.